Food Chemistry: X 16 (2022) 100454

Contents lists available at ScienceDirect

Food Chemistry: X

journal homepage: www.sciencedirect.com/journal/food-chemistry-x

Mechanistic understanding of the effect of zein–chlorogenic acid interaction on the properties of electrospun nanofiber films

Xinya Wang [a], Xiang Li [a], Jin Xue [a], Hao Zhang [a,*], Feng Wang [b,*], Jingsheng Liu [a]

[a] College of Food Science and Engineering, National Engineering Laboratory for Wheat and Corn Deep Processing, Jilin Agricultural University, Changchun 130118, PR China

[b] Key Laboratory of Rubber-Plastics, Ministry of Education/Shandong Provincial Key Laboratory of Rubber-plastics, Qingdao University of Science & Technology, Qingdao, 266042, China

ARTICLE INFO

Keywords:
Zein
Chlorogenic acid
Protein–polyphenol interaction
Electrospinning
Nanofiber film

Chemical compounds studied in this article:
Chlorogenic acid (PubChem CID:1794427)

ABSTRACT

The interaction mechanism between zein and chlorogenic acid (CA) and the effect of interaction on the performance of coaxial nanofiber films were investigated. The interactions between zein and CA were characterized by multiple spectroscopic methods. Ultraviolet spectrum analysis revealed the formation of a zein–CA complex. Fluorescence analysis pointed out that the quenching of zein by CA was static. FTIR and thermodynamic analyses showed that hydrogen bonds and electrostatic interactions dominated the interaction between zein and CA. Zein-based nanofiber films were successfully prepared by coaxial electrospinning. The interaction between zein and CA enhanced the mechanical properties but reduced the thermal stability of nanofiber films. The presence of CA endowed nanofiber films with antioxidant and antibacterial properties. This research provides significant insight into the effect of protein–polyphenol interactions on the properties of electrospun nanofiber films, which can be applied in the field of active packaging to improve food safety.

1. Introduction

Zein is present in corn endosperm and accounts for 44–79% of the total corn protein. It is the major protein in corn gluten meal, a co-product of corn starch produced by a wet process and a renewable resource (Glusac & Fishman, 2021). Zein is a safe, nontoxic, biocompatible, and biodegradable substance that is generally recognized as a safe (GRAS) natural biomacromolecule (Kasaai, 2018). It is commonly used as a base material for the preparation of nanofiber films (Xue et al., 2022) and nanoparticles (Li, Wei, Sun, & Xue, 2022). Also, zein can form complexes with polyphenols via non-covalent interactions (Wang et al., 2022). Most polyphenols have antibacterial and antioxidant functions, so combining zein with bioactive phenolic compounds to prepare edible active packaging has attracted great interest. Altan and Çayır (2020) studied zein nanofiber films encapsulated with carvacrol, and the results showed that the loading of carvacrol enhanced the thermal stability of the nanofiber films. Huang, Ge, Zhou & Wang(2022) encapsulated eugenol in zein-polylactic acid films and found that with the increase of eugenol concentration in films, the inhibition ability of films against *Escherichia coli* and *Staphylococcus aureus* increased. The zein-polylactic acid-eugenol film has the potential for active packaging.

Chlorogenic acid (CA), 3-o-caffeoylquinic acid, is a common polyphenol found in coffee beans and honeysuckle. Studies have confirmed that it has biological (antioxidant, antibacterial, and antiviral) activities (Sun et al., 2021), metal chelation (Milić et al., 2011) and other activities. It also prevents the degradation of other bioactive compounds (Kopjar, JakŠIĆ, & PiliŽOta, 2012). In recent years, to improve the bioavailability of CA and optimize the structural and functional properties of proteins, some scholars have studied the interaction mechanism of CA with proteins and their influences on protein conformation and properties. Zhang et al. (2021b) studied the interactions between whey proteins and CA and determined that CA had the highest binding affinity with α-lactalbumin, mainly through hydrophobic force. Using multispectral and molecular docking methods, Perumal, Marimuthu, and Chen (2021) found that the interaction between CA and ovalbumin reduced the content of α-helix structure of ovalbumin. Zhang et al. (2021a) found that the interaction between CA and gliadin and glutenin has a significant synergistic antioxidant effect.

Both zein and CA are derived from food and can be obtained in large quantities from by-products or food processing waste. Using them as materials to prepare active packaging can increase its added value, reduce production costs, and also reduce the environmental pollution

* Corresponding authors.
E-mail addresses: zhanghao3318@sina.com (H. Zhang), dr_fengwang@163.com (F. Wang).

https://doi.org/10.1016/j.fochx.2022.100454
Received 9 June 2022; Received in revised form 12 September 2022; Accepted 22 September 2022
Available online 23 September 2022

caused by traditional packaging materials. However, there are few reports on the interaction mechanism between zein and CA and the preparation of active packaging based on zein-CA interaction. In this study, the interaction mechanism between zein and CA was fully characterized using multiple spectra techniques. Based on this study, the effect of interactions on the properties of CA-loaded zein-based nanofiber films was further investigated, and the potential of the nanofiber films as active packaging materials was evaluated. This work may offer important information for research and development of low-cost and environmentally friendly active packaging, especially in the aspect of the mechanical, antioxidant, and antibacterial characteristics of packaging.

2. Materials and methods

2.1. Materials

Zein was obtained from Wako Pure Chemical Industries, ltd. (Tokyo, Japan). The crude protein content of zein was 84.4%. Chlorogenic acid (99.7% purity) was obtained from TmStandard (Beijing, China). DPPH (1,1-diphenyl-2-picrylhydrazyl) was obtained from Haoyuan (Shanghai, China) and ABTS (2,2′-azinobis-3-ethylbenzthiazoline-6-sulfonate) was obtained from Sigma-Aldrich (Sa. Louis, MO, USA). Other chemicals and reagents used were of analytical grade.

2.2. Preparation of complex

The zein-CA mixture was prepared with reference to the method of Wang et al. (2022) with some modifications. Both zein and CA powders were dissolved in an aqueous solution of ethanol 85% v/v. The two solutions were mixed in different ratios and vortexed for 20 min (the final zein concentration was 0.2 mg/mL and the CA concentration was 5–40 μM). Dissolution and mixing solutions were carried out in the dark at 25 °C.

2.3. UV–vis spectrum

The UV spectra were determined with reference to the procedure of Liu et al. (2017) with some modifications. A series of UV–vis spectroscopic measurements were performed on the zein, CA, and zein-CA solutions using a UV–vis spectrophotometer (UV-2600, Shimadzu, Japan) operating in the scanning range of 200–400 nm. A quartz cuvette with a path length of 1 cm was used for the test.

2.4. Fluorescence spectroscopy

The fluorescence spectra of the zein and zein–CA solutions were recorded using the fluorescence spectrophotometer (RF-5301PC, Shimadzu, Japan) at 25 °C, 30 °C, and 35 °C. The distribution of fluorescence intensity in the range of 290–450 nm was observed under excitation light of 280 nm. For both excitation and emission, a slit width of 3 nm was used. Each sample was scanned thrice to obtain an average value. A formula was used to adjust the fluorescence result to remove the inner-filter effects. (van de Weert & Stella, 2011).

$$F_c = F_0 \times e^{(A_{ex}+A_{em})/2} \quad (1)$$

where F_0 and F_c are the fluorescence intensities before and after correction. A_{ex} and A_{em} are the absorbances of CA at 280 nm and 304 nm, respectively.

2.5. FTIR spectroscopy

The zein–CA solution was then frozen and dried. Fourier transform infrared spectra (VERTEX-70, Bruker, America) were acquired using the method reported by Liu et al. (2021a). The scanning wavelength range was 4000–400 cm^{-1}, and the spectra were obtained at a resolution of 4 cm^{-1} with the co-addition of 32 scans. The samples (0.002 g) were blended with KBr (0.2 g). The mixtures were ground into a uniform powder under infrared light, and the film was formed after pressing for 1 min. As a baseline, pure KBr was tested.

2.6. CD spectra

The secondary structures of the zein and zein–CA solutions were analyzed using circular dichroism (J-820, Jasco, Japan), which covered a scanning range of 190–260 nm. The baseline was 85% (v/v) ethanol. We used the following equation (Tiwari, Ali, Ishrat, & Arfin, 2021) to express CD results based on residue ellipticity (MRE):

$$MRE_{208} = \frac{\text{observed CD (millidegree)}}{C_p\, n\, l \times 10} \quad (2)$$

In this equation, C_p is the molar concentration of the protein, n is the number of amino acid residues in zein (in this case 266), and L (0.1 cm) is the path length. The calculation equation for the α-helix content of the sample was as follows (Tiwari, Ali, Ishrat, & Arfin, 2021):

$$\alpha - helix(\%) = -\frac{[MRE_{208} - 4000]}{33000 - 4000} \times 100 \quad (3)$$

2.7. Preparation of electrospun films

The preparation of electrospun solutions and the production of nanofiber films were performed according to the method of Colussi, Ferreira da Silva, Biduski, Mello El Halal, da Rosa Zavareze, & Guerra Dias (2021) with some modifications. First, 25 wt% zein solution and 15 wt% polyvinylpyrrolidone (PVP) solution were prepared by stirring zein and PVP in 85% (v/v) ethanol–water for 2 h. The 25 wt% zein solution was mixed with CA in the dark for 30 min. In brief, the core solution contained 25 wt% zein with varying CA contents (0.5, 1.0, 1.5, and 2.0% w/w). Then, the shell solution was collected by blending a 25 wt% zein solution and a 15 wt% PVP solution at the same mass ratio for 30 min.

Coaxial electrospinning was used to obtain active nanofiber films. A syringe, a drum collector, and a high-voltage power source make up the electrospinning apparatus. The nanofibers were collected on tinfoil that covered the drum collector. The parameters of coaxial electrospinning were set as follows: applied voltage, 18 kV; collector speed, 1500 rpm; shell flow rate, 5 mL/h; core flow rate, 2 mL/h; and distance, 13 cm. The temperature and relative humidity in the experimental environment were maintained at 25 ± 2 °C and 50 ± 5%, respectively.

2.8. Thermal performances

The thermal properties of nanofiber films with zein alone and zein loaded with different CA contents were measured using differential scanning calorimetry (Q2000, TA, America) according to the procedure of Liu, Ma, McClements, and Gao (2017) with some modifications. Samples (4–5 mg) were weighed and heated in nitrogen at a rate of 10 °C min^{-1} from 20 °C to 250 °C.

2.9. Mechanical performances

With reference to the method of Yao, Gao, Chen, and Du (2022), the mechanical properties of the nanofiber films were measured using a texture analyzer (INSIRON-5869, Instron, America) according to the GB/T 1040.1-2006 protocol. The nanofiber films were sliced into 10 mm × 50 mm strips. Each nanofiber film was sliced into three uniform strips for measurement. The crosshead speed of the instrument was 10 mm/min, and the clamping distance was 20 mm.

2.10. Antioxidant capacity

The scavenging ability of nanofiber films with different CA contents to DPPH and ABTS free radicals can characterize their antioxidant capacity. For testing, 10 mg of nanofiber films were dissolved in 1 mL of 85% (v/v) ethanol–water for 1 h as the sample solution.

Some minor modifications were made in reference to Neo et al. (2013). The supernatant of the sample was blended with DPPH solution in a ratio of 1:30, and then stored in an opaque box for 15 min. A measurement of the absorbance was made at 517 nm.

According to the method of Colussi, Ferreira da Silva, Biduski, Mello El Halal, da Rosa Zavareze, and Guerra Dias (2021), potassium persulfate and ABTS were combined in equal proportion and reacted in darkness for 12 h. The supernatant of the sample was mixed with the ABTS diluent at a ratio of 1:20 and left to react for 15 min in an opaque box before the absorbance at 734 nm was recorded.

ABTS and DPPH solutions without nanofiber films were used as controls. The results were determined as:

$$\text{Radical scavenging activity}(\%) = \frac{A_{control} - A_{sample}}{A_{control}} \times 100 \quad (4)$$

2.11. Antimicrobial activity

The nanofiber films were tested for their antimicrobial activity against *Staphylococcus aureus (S. aureus)* by using the agar plate diffusion method (Kang et al., 2017). The nanofiber films were made into circular pieces with a diameter of 6 mm. For disinfection, the samples were irradiated with UV light for 30 min before use. Sterilized nanofiber films were glued to the agar medium and incubated in a 37 °C incubator for 24 h. The antibacterial ability of the nanofiber films was assessed based on the size of the inhibition zone.

2.12. Statistical analysis

Three times were repeated in all experiments. All charts were drawn using Origin, and statistical analyses were conducted using the SPSS software. The test results are showed as a mean ± standard deviation. The statistical significance was set at $p < 0.05$.

3. Results and discussion

3.1. UV spectrum

UV spectroscopy is a credible tool to detect the formation of new complexes. Fig. 1A shows the UV absorption spectra of zein, CA, and zein–CA. Zein displayed strong absorption peaks at 210 nm and 278 nm, respectively. Zein's absorption peak at 278 nm was because of the aromatic ring's π–π* transition on the tyrosine residue (Liu et al., 2021a). The absorption peaks of CA are located at 302 and 330 nm, respectively. The absorbance of the zein-CA was higher than that of the same concentration of CA and zein. In addition, zein's absorption peak at 278 nm increased with increasing CA content while experiencing a red shift. In summary, all the results indicated that CA interacted with zein to form the zein-CA complex and that the interaction changed the tertiary structure of zein (Zhong, Zhao, Dai, McClements, & Liu, 2021).

3.2. Fluorescence spectroscopy

Fluorescence spectroscopy is an efficient technique for exploring interactions between zein and CA. The quenching mechanism, binding sites, binding constants, and types of binding forces between proteins and polyphenols can be analyzed using the fluorescence quenching data (Xu, Hao, Sun, & Tang, 2019). Zein has a high concentration of tyrosine residues but a substantially lower concentration of tryptophan residues; as a result, its typical maximum fluorescence peak is approximately 304 nm (Shukla & Cheryan, 2001). At different temperatures, zein interacting with CA results in the fluorescence quenching spectra shown in Fig. 1B–D. Increasing the CA concentration at three different temperatures caused a gradual decrease in the fluorescence intensity at the wavelength of 304 nm. This phenomenon effectively proves that CA has a fluorescence-quenching effect on zein. Generally, the fluorescence

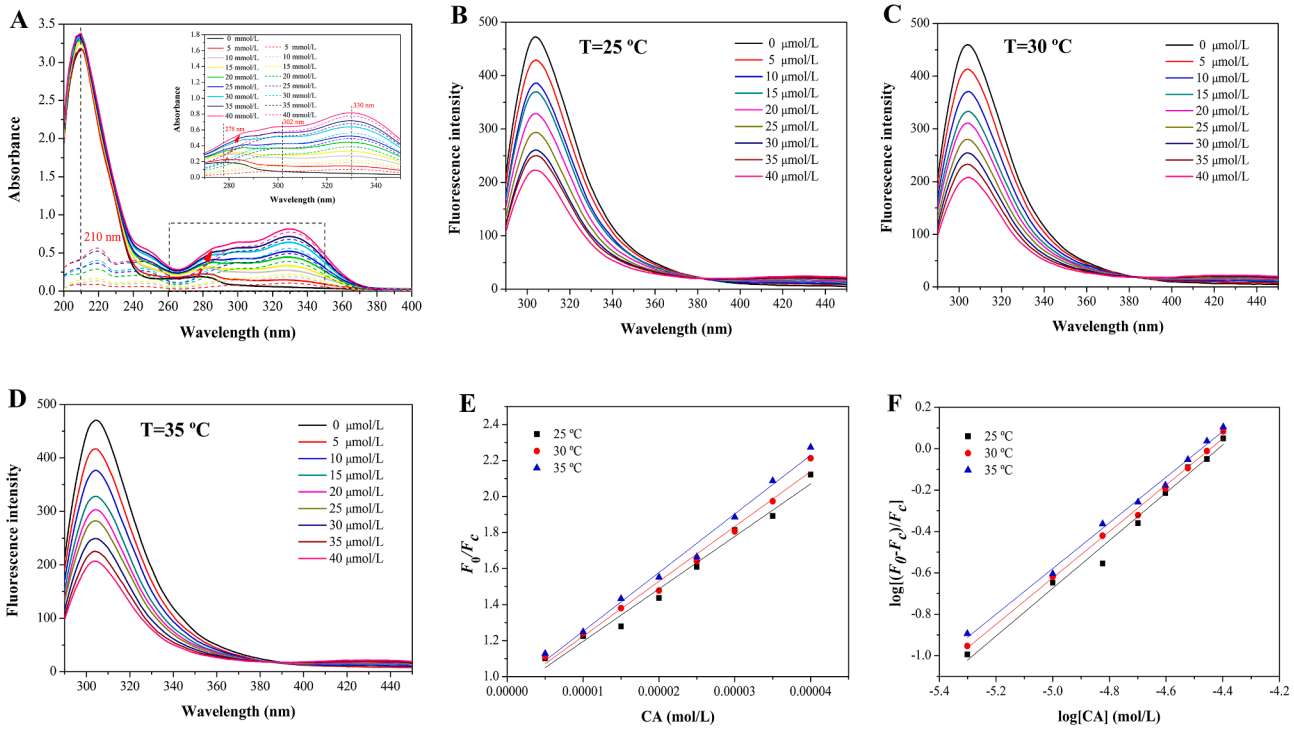

Fig. 1. A: UV–vis absorption spectra of zein, CA, and zein–CA; B: Fluorescence spectra of zein–CA at 25 ℃; C: Fluorescence spectra of zein–CA at 30 ℃; D: Fluorescence spectra of zein–CA at 35 ℃; E: Stern–Volmer plots of zein–CA at different temperatures; F: Double logarithmic plots of zein-CA at different temperatures.

quenching mechanism can be divided into static quenching and dynamic quenching, and the quenching mechanism can be judged by the quenching rate constant K_q. To deeply explore the quenching mechanisms between zein and CA, the Stern–Volmer equation was adopted.

$$F_0/F_c = 1 + K_q\tau_0[Q] = 1 + K_{sv}[Q] \quad (5)$$

where K_q is the quenching rate constant, τ_0 is the average lifetime of molecules without CA, generally 10^{-8} s; [Q] is the concentration of CA, and K_{sv} is the quenching constant. Fig. 1E shows the Stern-Volmer curves at various temperatures. The relationship between F_0/F_c and [Q] was linear (R^2 = 0.980, 0.985, and 0.989). Based on the slope of the equation, K_{sv} values were calculated. At 25 ℃, 30 ℃, and 35 ℃ the K_{sv} values were 2.92 × 10^4 L mol^{-1}, 3.05 × 10^4 L mol^{-1}, and 3.26 × 10^4 L mol^{-1} respectively, and gradually increased with increasing temperature. K_q was 2.92 × 10^{12} L $mol^{-1}{\cdot}s^{-1}$, 3.05 × 10^{12} L $mol^{-1}{\cdot}s^{-1}$, and 3.26 × 10^{12} L $mol^{-1}{\cdot}s^{-1}$. The maximum dynamic quenching rate constant (2 × 10^{10} L $mol^{-1}{\cdot}s^{-1}$) was lower than the minimum K_q. The results were similar to those of Zhong (Zhong, Zhao, Dai, McClements, & Liu, 2021), and it could be concluded that the quenching mode of zein–CA was static quenching. The binding constants and binding sites of zein–CA were obtained by the double logarithmic equation:

$$\log\left[\frac{F_0 - F_c}{F_c}\right] = \log K_a + n\log[Q] \quad (6)$$

where K_a is the binding constant between zein and CA, and n is the number of binding sites. The results obtained from this equation can be found in Table 1. At different temperatures, the numbers of binding sites between zein and CA were all approximately equal to 1, suggesting that only one CA molecule was bound to each zein molecule. Moreover, the binding constant between proteins and polyphenols was an important indicator of their affinity. The value of K_a gradually decreased from 1.24 × 10^5 L mol^{-1} to 0.87 × 10^5 L mol^{-1} as the temperature was raised, indicating that the affinity between zein and CA was weaker at higher temperatures. Calculation of thermodynamic parameters for the interaction between zein and CA using the van 't Hoff equation:

$$RlnK = \Delta S - \Delta H/T \quad (7)$$

$$\Delta G = \Delta H - T\Delta S = -RT\,lnK \quad (8)$$

where R is the gas constant (8.314 J mol^{-1} K^{-1}). T is the absolute temperature. ΔH, ΔS, and ΔG can be obtained from this equation, and the results can be found in Table 1. Proteins can interact with small molecules through hydrophobic interactions, hydrogen bonding, electrostatic interactions, and van der Waals forces. The type of non-covalent interaction between protein and small molecule can be judged by the magnitude of thermodynamic parameters. The negative value of the Gibbs free energy change (ΔG) suggested the spontaneity of the interaction between zein and CA. According to the conclusion of Wang et al. (2021), $\Delta S > 0$ and $\Delta H < 0$, indicating a significant role for electrostatic interactions in binding zein to CA.

Table 1
The binding constant K_a, number of binding sites n and thermodynamic parameters ΔH, ΔS and ΔG of zein–CA at different temperatures.

System	T (℃)	n	K_a (10^5 L mol^{-1})	ΔH (kJ/mol)	ΔS (J/mol·K)	ΔG (kJ/mol)
zein-CA	25	1.15	1.24	−2.736	2.527	−3.489
	30	1.12	0.97			−3.504
	35	1.10	0.87			−3.519

3.3. FTIR spectroscopy

FTIR is used to analyze the interactions between molecules. It has the characteristics of fast testing speed, high sensitivity, and low sample consumption. Diagram 2A shows the Fourier transform infrared spectra of zein, CA, and their mixed systems. The absorption of natural zein powder at 3415 cm^{-1} corresponds to the O—H stretching vibration. The absorption peak at 1639 cm^{-1} of the amide I band corresponded to C═O stretching, and the absorption peak at 1544 cm^{-1} of the amide II band was due to C—N stretching and N—H bending vibration (Yin, Yang, Zhao, & Li, 2014). When zein was combined with CA, the absorption peak at 3415 cm^{-1} was transferred to 3311 cm^{-1}, indicating the formation of a hydrogen bond between zein and CA. The changes of 1639 cm^{-1} and 1544 cm^{-1} to 1656 cm^{-1} and 1541 cm^{-1} revealed that there was electrostatic interaction between zein and CA, respectively. These results were consistent with the interaction between zein and quercetin previously reported by Sun et al. (2015).

3.4. CD spectra

The effects of small molecules on the secondary structure of the protein were researched using CD spectra. The CD spectra of zein shows two negative peaks at 208 and 221 nm, which are classic α-helix peaks, as seen in Fig. 2B (Gordon, Sharon, & David, 2007). The negative peak at 208 nm was put down to π–π* transitions. The negative peak at 221 nm might be resulted from n–π* transitions of the α-helix and random coil (Tan, Zhou, Guo, Zhang, & Ma, 2021). The binding of CA caused a decrease in the band of natural zein at 208 nm and 221 nm. This clearly indicates a diminution in the content of α-helix structure in zein. According to Eqs. (2) and (3), the α-helix content of natural zein was 61.15%. The α-helix content of zein was reduced from 59.54% to 57.59% upon binding to 20 μM CA and 40 μM CA respectively. The results show that the presence of CA changed the secondary structure of zein. This might be because of electrostatic interactions and hydrogen bonding between the hydroxyl groups on the benzene ring of CA and amino acid residues on the zein surface (Liu et al., 2007). These results imply that the interaction of zein with CA leads to slight conformational changes in the protein. When studying the binding mechanism of CA and the whey protein, Zhang et al. (2014) found that the α-helix structure of β-lactoglobulin was also lessened following the interaction between CA and β-lactoglobulin. A decrease in the α-helix content of the protein may indicate a partial unfolding of the protein structure, which would make it less stable.

3.5. Thermal performances

The thermal performance of all coaxial nanofiber films was analyzed by DSC, and the results are depicted in Fig. 3A. As the denaturation of the nanofiber films was linked to the three-dimensional structure of zein, we only concentrated on this process in our work. Previously, Liu, Ma, McClements, and Gao (2017) reported that the thermal denaturation temperature (T_d) of zein was 91.5 °C. However, the T_d of the zein based nanofiber film obtained here was quite different. The difference in T_d may result from the use of different zein sources and the addition of PVP. As indicated in Fig. 3A, the T_d of the nanofiber films was reduced with increasing CA content ($P < 0.05$), among which the T_d of the nanofiber film without CA was the highest (121.73 ± 2.5 ℃). The T_d of the nanofiber film containing 2.0% CA, on the other hand, decreased by 14 °C. The T_d of the nanofiber films loaded with CA was lower than that without CA. The addition of CA reduced the α-helix content of zein as determined by CD. Therefore, the decrease in T_d may be ascribed to the hydrogen bonding and electrostatic interactions between CA and zein, which induced disorder in the system and weakened the thermal stability of coaxial nanofiber films (Li et al., 2021).

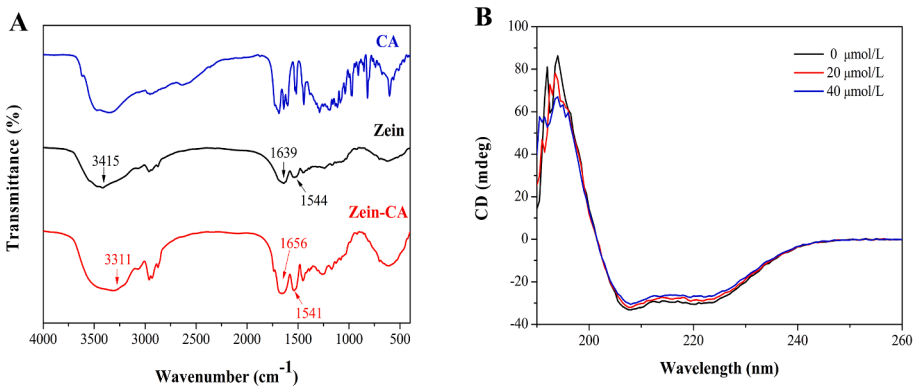

Fig. 2. A: FTIR spectra of CA, zein and zein–CA; B: CD spectra of zein and zein–CA with different concentrations of CA.

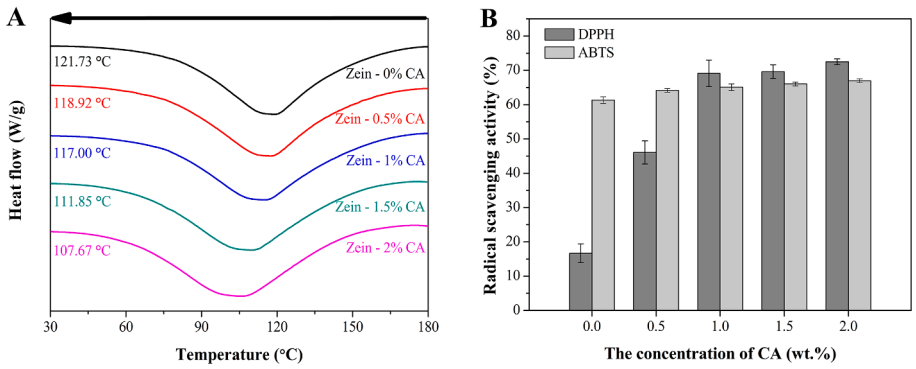

Fig. 3. A: DSC curves of nanofiber films with different CA additions; B: Antioxidant activity of nanofiber films with different CA additions.

3.6. *Mechanical performances*

Mechanical strength and tensile properties of packaging materials are essential in food packaging. Fig. 4A shows the stress–strain curves of coaxial nanofiber films with various CA contents. The mechanical properties of the coaxial nanofiber films steadily improved as the CA

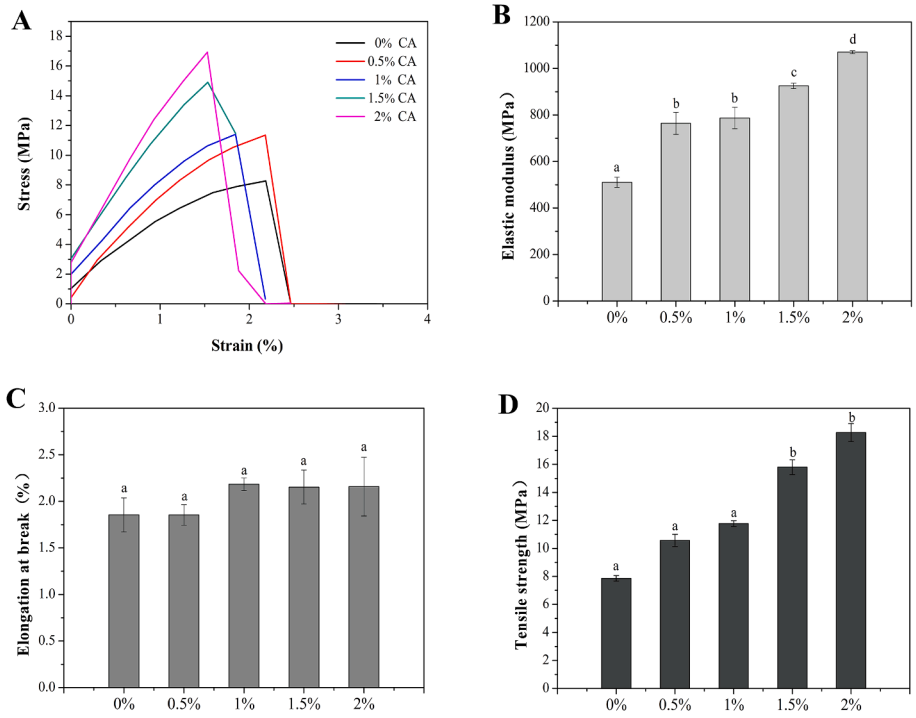

Fig. 4. Mechanical properties of nanofiber films with different CA additions: (A) stress–strain curves; (B) elastic modulus; (C) elongation at break; and (D) tensile strength.

content of the core solution increased. Fig. 4B, C, and D show the elastic modulus, elongation at break, and tensile strength of coaxial nanofiber films with different CA contents. The elastic modulus of the coaxial nanofiber films increased from 510 to 1070 MPa with increasing CA content, suggesting an enhanced resistance against film deformation. The addition of CA enhanced the rigidity and brittleness of the coaxial nanofiber films ($P < 0.05$). Phenol-protein interchain interactions reduced the influence of the plasticizer within the film, resulting in increased rigidity. Similar results were reported by Nie, Gong, Wang, and Meng (2015). In coaxial nanofiber films without CA, the elongation at break was 1.85% and the tensile strength was 7.86 MPa. The elongation at break of the nanofiber films initially increased and then decreased with increasing CA addition, reaching the highest value (2.18%) when the CA addition was 1.0%, and decreasing to the lowest value (2.15%) when the CA content was 2.0%, but the change was not significant ($P > 0.05$). When 0.5–2.0% CA was added to the core solution, the tensile strength increased gradually from 10.57 MPa to 18.27 MPa ($P < 0.05$). The tensile strength of zein nanofiber film with 2.0% CA increased by 132.44%. The above results are caused by hydrogen bonds formed between the carboxyl groups of zein and the hydroxyl groups of CA, which enhance the interactions between zein molecules (Zhang et al., 2021). This was further confirmed using FTIR and CD analysis. These interactions contribute to a more dense structure, hence improving the tensile strength of the nanofiber films. The pomelo peel flour–based films with tea polyphenols prepared by Wu et al. (2019) showed a similar result. The addition of polyphenols could significantly improve the tensile strength of nanofiber films, which might be used as packaging materials.

3.7. Antioxidant capacity

In Fig. 3B, the antioxidant capacity of nanofiber films was assessed using DPPH and ABTS scavenging assays. The scavenging rates of DPPH and ABTS free radicals by the zein-based nanofiber film without CA were 16% and 61%, respectively. This was due to the antioxidant properties of zein (Zhang, Luo, & Wang, 2011). With an increase in the CA content, the DPPH and ABTS scavenging abilities of zein-based nanofiber films increased from 46% to 72% and 64% to 66%, respectively, and reached the highest values when the CA content was at 2.0%. In conclusion, the total antioxidant capacities of the zein-based nanofiber films considerably increased ($P < 0.05$) as the CA content of the films multiplied. This indicates that CA was successfully encapsulated in the nanofiber film. For effective application of nanofiber films as active packaging to ensure the quality of food, the antioxidant capacity of coaxial nanofiber films can be optimized by adjusting the amount of added CA.

3.8. Antimicrobial activity

The antimicrobial activity test is an indicator to evaluate zein-based nanofiber films loaded with chlorogenic acid as an active packaging material. Retail food products are particularly susceptible to contamination by *S. aureus*, which can cause foodborne poisoning. In China, foodborne bacterial outbreaks caused by *S. aureus* were reported to account for about 20%-25% of the total. As shown in Fig. 5, the zein-based nanofiber film without CA loading did not show any inhibition zone for *S. aureus*, indicating that zein and PVP had no antimicrobial activity. When 0.5%, 1.0%, 1.5%, and 2.0% CA were added to the zein-based nanofiber films, inhibition zones appeared near the nanofiber film, indicating that the nanofiber film loaded with CA had an inhibitory effect on *S. aureus*. However, all nanofiber films loaded with CA presented small inhibition zones for *S. aureus* (Fig. 5). The sizes of the inhibition zones of the nanofiber films with 0.5%, 1.0%, and 1.5% CA were similar, whereas the inhibition zone of the nanofiber film with 2.0% CA was slightly larger than that of the other groups. The antimicrobial activities of the nanofiber films were related to the CA content and the distance of CA from the inside of the fiber to the surface (Kang et al., 2017). Even though the size of the inhibition zone of CA-loaded zein-based nanofiber films against *S. aureus* in this study was small, it can still be demonstrated that the loading of CA can make zein-based nanofiber films have antibacterial effect against *S. aureus* and can be used as a potential active food packaging material.

4. Conclusions

A multispectral method was used to research the interaction between zein and CA in this paper. The UV spectra demonstrated that CA interacted with zein to form the zein-CA complex. The fluorescence spectra showed that the quenching mode of CA for zein was static quenching and that the spontaneous binding of CA and zein was fueled by electrostatic interactions. The binding of CA to zein was demonstrated by infrared spectra to have been primarily mediated by hydrogen bonds and electrostatic interactions. Based on circular dichroism analysis, zein's secondary structure was altered by its interaction with CA. In addition, zein was mixed with PVP as a shell solution and with various concentrations of CA as the core solution for coaxial electrostatic spinning. The effect of the interaction between zein and CA on the properties of nanofiber films was studied. The results show that CA was successfully encapsulated in the nanofibers, which existed in the form of continuous non-beaded shell cores. The interaction between zein and CA reduced the thermal stability, augmented the mechanical properties and antioxidant capacity of the nanofiber films, and improved their antibacterial effect. In this study, CA and zein were combined and encapsulated in

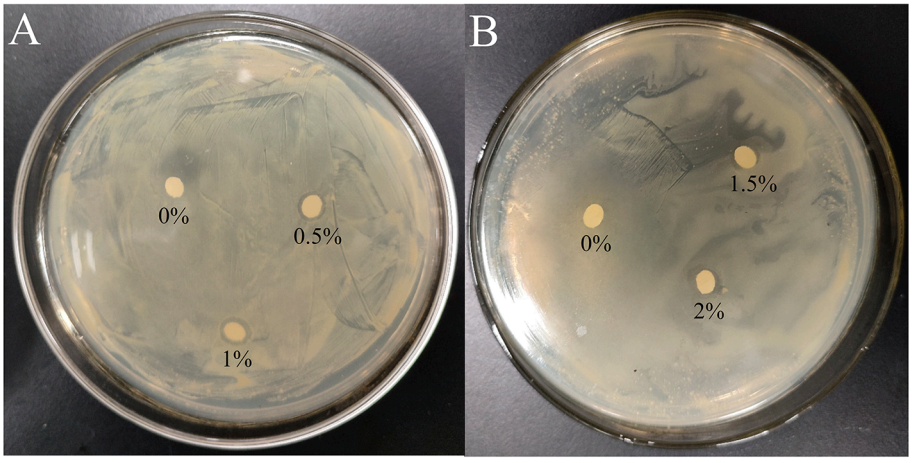

Fig. 5. Antimicrobial activity of nanofiber films with different CA additions.

nanofibers, revealing the influence of the interaction between zein and CA on the physicochemical and functional properties of nanofiber films. Our findings offer an effective solution for the comprehensive utilization of plant protein and plant active ingredients and provide new ideas for the exploitation of low-cost and environmentally friendly active packaging.

CRediT authorship contribution statement

Xinya Wang: Conceptualization, Data curation, Methodology, Investigation, Software, Visualization, Validation, Writing – original draft. **Xiang Li:** Investigation, Visualization. **Jin Xue:** Investigation. **Hao Zhang:** Writing – review & editing, Resources, Supervision, Funding acquisition. **Feng Wang:** Visualization, Writing – review & editing. **Jingsheng Liu:** Supervision, Resources.

Declaration of competing interest

The authors declare that they have no known competing financial interests or personal relationships that could have appeared to influence the work reported in this paper.

Data availability

The data that has been used is confidential.

Acknowledgements:

The authors of this study sincerely thank the financial support provided by the National Natural Science Foundation of China (32072169, 31801477).

Ethical statement

Ethics approval was not required for this research.

References:

Altan, A., & Çayır, Ö. (2020). Encapsulation of carvacrol into ultrafine fibrous zein films via electrospinning for active packaging. *Food Packaging and Shelf Life, 26*, Article 100581. https://doi.org/10.1016/j.fpsl.2020.100581

Colussi, R., Ferreira da Silva, W. M., Biduski, B., Mello El Halal, S. L., da Rosa Zavareze, E., & Guerra Dias, A. R. (2021). Postharvest quality and antioxidant activity extension of strawberry fruit using allyl isothiocyanate encapsulated by electrospun zein ultrafine fibers. *LWT - Food Science and Technology, 143*, Article 111087. https://doi.org/10.1016/j.lwt.2021.111087

Glusac, J., & Fishman, A. (2021). Enzymatic and chemical modification of zein for food application. *Trends in Food Science & Technology, 112*, 507–517. https://doi.org/10.1016/j.tifs.2021.04.024

Gordon, W. S., S. A. H. H., & David J. S. (2007). Effect of solvent and temperature on secondary and tertiary structure of zein by circular dichroism. Cereal Chemistry, 84 (3), 265-270. https://doi.org/10.1094/ CCHEM-84-3-0265.

Huang, X., Ge, X., Zhou, L., & Wang, Y. (2022). Eugenol embedded zein and poly(lactic acid) film as active food packaging: Formation, characterization, and antimicrobial effects. *Food Chemistry, 384*, Article 132482. https://doi.org/10.1016/j.foodchem.2022.132482

Kang, W., Ju, J., Zhao, H., Li, Z., Ma, X., & Cheng, B. (2017). Characterization and antibacterial properties of Ag NPs doped nylon 6 tree-like nanofiber membrane prepared by one-step electrospinning. *Fibers and Polymers, 17*(12), 2006–2013. https://doi.org/10.1007/s12221-016-6821-0

Kasaai, M. R. (2018). Zein and zein -based nano-materials for food and nutrition applications: A review. *Trends in Food Science & Technology, 79*, 184–197. https://doi.org/10.1016/j.tifs.2018.07.015

Kopjar, M., JakŠIĆ, K., & PiliŽOta, V. (2012). Influence of sugars and chlorogenic acid addition on anthocyanin content, antioxidant activity and color of blackberry juice during storage. *Journal of Food Processing and Preservation, 36*(6), 545–552. https://doi.org/10.1111/j.1745-4549.2011.00631.x

Li, D., Wei, Z., Sun, J., & Xue, C. (2022). Tremella polysaccharides-coated zein nanoparticles for enhancing stability and bioaccessibility of curcumin. *Current Research in Food Science, 5*, 611–618. https://doi.org/10.1016/j.crfs.2022.03.008

Li, M., Yu, H., Xie, Y., Guo, Y., Cheng, Y., Qian, H., & Yao, W. (2021). Fabrication of eugenol loaded gelatin nanofibers by electrospinning technique as active packaging material. *LWT - Food Science and Technology, 139*. https://doi.org/10.1016/j.lwt.2020.110800

Liu, C., Lv, N., Ren, G., Wu, R., Wang, B., Cao, Z., & Xie, H. (2021). Explore the interaction mechanism between zein and EGCG using multi-spectroscopy and molecular dynamics simulation methods. *Food Hydrocolloids, 120*, Article 106906. https://doi.org/10.1016/j.foodhyd.2021.106906

Liu, F., Ma, C., McClements, D. J., & Gao, Y. (2017). A comparative study of covalent and non-covalent interactions between zein and polyphenols in ethanol-water solution. *Food Hydrocolloids, 63*, 625–634. https://doi.org/10.1016/j.foodhyd.2016.09.041

Liu, M., Zhu, L. Y., Qu, X. K., Sun, D. Z., Li, L. W., & Lin, R. S. (2007). Studies on the binding of paeonol and two of its isomers to human serum albumin by using microcalorimetry and circular dichroism. *The Journal of Chemical Thermodynamics, 39*(12), 1565–1570. https://doi.org/10.1016/j.jct.2007.05.003

Milić, S. Z., Potkonjak, N. I., Gorjanović, S.Ž., Veljović-Jovanović, S. D., Pastor, F. T., & Sužnjević, D.Ž. (2011). A polarographic study of chlorogenic acid and its interaction with some heavy metal ions. *Electroanalysis, 23*(12), 2935–2940. https://doi.org/10.1002/elan.201100476

Neo, Y. P., Ray, S., Jin, J., Gizdavic-Nikolaidis, M., Nieuwoudt, M. K., Liu, D., & Quek, S. Y. (2013). Encapsulation of food grade antioxidant in natural biopolymer by electrospinning technique: A physicochemical study based on zein-gallic acid system. *Food Chemistry, 136*(2), 1013–1021. https://doi.org/10.1016/j.foodchem.2012.09.010

Nie, X., Gong, Y., Wang, N., & Meng, X. (2015). Preparation and characterization of edible myofibrillar protein-based film incorporated with grape seed procyanidins and green tea polyphenol. *LWT - Food Science and Technology, 64*(2), 1042–1046. https://doi.org/10.1016/j.lwt.2015.07.006

Perumal, M., Marimuthu, P., & Chen, X. (2021). Investigation into the site-specific binding interactions between chlorogenic acid and ovalbumin using multi-spectroscopic and in silico simulation studies. *Journal of Biomolecular Structure and Dynamics, 1–15*. https://doi.org/10.1080/07391102.2021.1886992

Shukla, R., & Cheryan, M. (2001). Zein: The industrial protein from corn. *Industrial Crops and Products, 13*(2001), 171–192. https://doi.org/10.1016/S0926-6690(00)00064-9

Sun, C., Yang, J., Liu, F., Yang, W., Yuan, F., & Gao, Y. (2015). Effects of dynamic high-pressure microfluidization treatment and the presence of quercetagetin on the physical, structural, thermal, and morphological characteristics of zein nanoparticles. *Food and Bioprocess Technology, 9*(2), 320–330. https://doi.org/10.1007/s11947-015-1627-4

Sun, J., Wang, D., Sun, Z., Liu, F., Du, L., & Wang, D. (2021). The combination of ultrasound and chlorogenic acid to inactivate staphylococcus aureus under planktonic, biofilm, and food systems. *Ultrasonics Sonochemistry, 80*, Article 105801. https://doi.org/10.1016/j.ultsonch.2021.105801

Tan, H., Zhou, H., Guo, T., Zhang, Y., & Ma, L. (2021). Integrated multi-spectroscopic and molecular modeling techniques to study the formation mechanism of hidden zearalenone in maize, 129286–129286 *Food Chemistry, 351*. https://doi.org/10.1016/j.foodchem.2021.129286.

Tiwari, P., Ali, R., Ishrat, R., & Arfin, N. (2021). Study of interaction between zein and curcumin using spectroscopic and in silico techniques. *Journal of Molecular Structure, 1230*, Article 129637. https://doi.org/10.1016/j.molstruc.2020.129637

Van de Weert, M., & Stella, L. (2011). Fluorescence quenching and ligand binding: A critical discussion of a popular methodology. *Journal of Molecular Structure, 998* (1–3), 144–150. https://doi.org/10.1016/j.molstruc.2011.05.023

Wang, H., Xia, X., Yin, X., Liu, H., Chen, Q., & Kong, B. (2021). Investigation of molecular mechanisms of interaction between myofibrillar proteins and 1-heptanol by multiple spectroscopy and molecular docking methods. *International Journal of Biological Macromolecules, 193*, 672–680. https://doi.org/10.1016/j.ijbiomac.2021.10.105

Wang, Q., Tang, Y., Yang, Y., Lei, L., Lei, X., Zhao, J., … Ming, J. (2022). The interaction mechanisms, and structural changes of the interaction between zein and ferulic acid under different pH conditions. *Food Hydrocolloids, 124*, Article 107251. https://doi.org/10.1016/j.foodhyd.2021.107251

Wu, H., Lei, Y., Zhu, R., Zhao, M., Lu, J., Xiao, D., … Li, S. (2019). Preparation and characterization of bioactive edible packaging films based on pomelo peel flours incorporating tea polyphenol. *Food Hydrocolloids, 90*, 41–49. https://doi.org/10.1016/j.foodhyd.2018.12.016

Xu, J., Hao, M., Sun, Q., & Tang, L. (2019). Comparative studies of interaction of beta-lactoglobulin with three polyphenols. *International Journal of Biological Macromolecules, 136*, 804–812. https://doi.org/10.1016/j.ijbiomac.2019.06.053

Xue, J., Li, X., Jin, X., Wang, X., Zhen, N., Song, T., … Liu, J. (2022). Electrocatalytic oxidation of formaldehyde using electrospinning porous zein-based polyimide fibers. *Materials Letters, 320*, Article 132318. https://doi.org/10.1016/j.matlet.2022.132318

Yao, F., Gao, Y., Chen, F., & Du, Y. (2022). Preparation and properties of electrospun peanut protein isolate/poly-l-lactic acid nanofibers. *LWT - Food Science and Technology, 153*, Article 112418. https://doi.org/10.1016/j.lwt.2021.112418

Yin, C., Yang, L., Zhao, H., & Li, C. P. (2014). Improvement of antioxidant activity of egg white protein by phosphorylation and conjugation of epigallocatechin gallate. *Food Research International, 64*, 855–863. https://doi.org/10.1016/j.foodres.2014.08.020

Zhang, B., Luo, Y., & Wang, Q. (2011). Effect of acid and base treatments on structural, rheological, and antioxidant properties of α-zein. *Food Chemistry, 124*(1), 210–220. https://doi.org/10.1016/j.foodchem.2010.06.019

Zhang, D., Chen, L., Cai, J., Dong, Q., Din, Z. U., Hu, Z. Z., … Cheng, S. Y. (2021). Starch/tea polyphenols nanofibrous films for food packaging application: From facile construction to enhance mechanical, antioxidant and hydrophobic properties. *Food Chemistry, 360*, Article 129922. https://doi.org/10.1016/j.foodchem.2021.129922

Zhang, H., Yu, D., Sun, J., Guo, H., Ding, Q., Liu, R., & Ren, F. (2014). Interaction of milk whey protein with common phenolic acids. *Journal of Molecular Structure, 1058*, 228–233. https://doi.org/10.1016/j.molstruc.2013.11.009

Zhang, K., Wen, Q., Li, T., Liu, Q., Wang, Y., & Huang, J. (2021a). Comparison of interaction mechanism between chlorogenic acid/luteolin and glutenin/gliadin by

multi-spectroscopic and thermodynamic methods. *Journal of Molecular Structure, 1246*. https://doi.org10.1016/j.molstruc.2021.131219.

Zhang, Y., Lu, Y., Yang, Y., Li, S., Wang, C., Wang, C., & Zhang, T. (2021b). Comparison of non-covalent binding interactions between three whey proteins and chlorogenic acid: Spectroscopic analysis and molecular docking. *Food Bioscience, 41*, Article 101035. https://doi.org/10.1016/j.fbio.2021.101035

Zhong, Y., Zhao, J., Dai, T., McClements, D. J., & Liu, C. (2021). The effect of whey protein-puerarin interactions on the formation and performance of protein hydrogels. *Food Hydrocolloids, 113*. https://doi.org/10.1016/j.foodhyd.2020.106444